Coherence and Information in a Fibre Interferometer

Part II E1
HoC: Tijmen Euser
Department of Physics
University of Cambridge

November 2021

Abstract

A Mach-Zehnder interferometer was used to investigate fringe contrast over a range of optical path lengths. Spectra of both SLD and Fabry-Perot laser sources were found and they closely matched those of the manufacturers handbook. Spatial coherence was also found to be $50 \pm 5\mu m$ for the SLD and was too large to calculate for the over our range Fabry-Perot. Contrast-gain plots were found for Erbium-doped fibre amplifiers in one/both of the arms where it was found that photon generated by spontaneous emission could contribute to interference patterns. A first-order noise model fit the data well. The velocity of a loudspeaker was found to be $v = 4mm * \sin(2\pi * 5\text{Hz} * t)$ by finding the Doppler shift of windowed Fourier transforms, amplitude-time was then found via Riemann integral. Total words: 2978

1 Introduction

The Mach-Zehnder interferometer is named after Ludwig Zehnder who proposed the apparatus in 1891 [6] and Ludwig Mach who refined it (1892) [4]. Consisting of two beams, it quantifies changes in optical path difference (OPD) and coherence using fringe contrast.

Here, the MZ interferometer allows for the deduction of spectra for two different sources. Erbium-doped fibre amplifier(s) were also added to one/both arm(s) to investigate the whether photons via stimulated emission can contribute to interference and how noise changes with gain. Finally the amplitude and velocity of a mirror attached to a loudspeaker were deduced using Doppler shift principles in laser vibrometry. Derivations that are not essential to understanding, are in the appendix.

2 Theory

2.1 Interference

Consider Ψ, the superposition of two monochromatic waves of angular frequency ω_1 and ω_2. Where $I \propto \Psi^2$ and $\psi = ae^{i\phi}$

$$\Psi = \Re[\psi_1 e^{-i\omega_1 t} + \psi_2 e^{-i\omega_2 t}] \tag{1}$$

When expanding I^2 and taking the time average, we know that the angular frequencies of the signals are on order 10^{14}Hz, which is much greater than the sampling rate of the detector, $1/\tau$,

where τ is the detector integration time, so terms depending of ω_1 or ω_2 only will time average to zero.

$$\langle I \rangle \propto \frac{1}{2}\langle a_1^2 \rangle + \frac{1}{2}\langle a_2^2 \rangle + \langle a_1 a_2 \Re[e^{i[\Delta\phi - (\omega_1 - \omega_2)t]}] \rangle \tag{2}$$

Where $\Delta\phi = \phi_1 - \phi_2$ is the phase difference between the two arms. This contains a time-independent term due to the delay line, $\Delta\phi'$ and a time-dependent term due to the modulator, $\Delta\phi''(t)$ where $|\Delta\phi'| >> |\Delta\phi''(t)|$.

Interference occurs when the final term is non-zero. If $(\omega_1 - \omega_2)\tau >> 1$, this third term will also time average to zero, so ω_1 and ω_2 must be close in value for interference to happen.

Fringe contrast/visibility is a quantitative measure of coherence between the beams:

$$C(x) = \frac{I(x+x')_{\max} - I(x+x')_{\min}}{I(x+x')_{\max} + I(x+x')_{\min}} = \frac{\text{peak-to-peak}}{2 * \text{mean}} \tag{3}$$

Using 2 and 3 and letting $a_1 = ka_2$ we can see that the maximum contrast, derived in section **??** for a given power ratio is:

$$\frac{2k}{1+k^2} \tag{4}$$

The contrast is related to the spectrum of the source via the equation [1]:

$$C(x) = \frac{2\sqrt{I_1 I_2} FT[S(\nu - \nu_0)]}{I_1 + I_2} \tag{5}$$

The spectrum is then found by taking the Fourier transform of the contrast.

2.2 Fourier methods

There is a reciprocal relationship between functions and their Fourier transforms. Narrow functions have wide Fourier transforms and wide functions have narrow Fourier transforms. Using this idea, if the spacings between measurements are small enough, the assumption of continuous measurement can be made. If continuous measurements are taken over a finite sized range, size w, the spectrum seen will only be an approximation, of the true spectrum this uncertainty can be quantified using convolution theory. Working and justification found in the appendix.

$$\frac{\Delta\lambda}{\lambda} = \frac{\lambda}{w} \tag{6}$$

This equation can be used to find the required sampling window for a desired spectral resolution. For example if we want to be able to resolve peak 1nm for 1550nm centred light the width would be $\frac{\lambda^2}{\Delta\lambda} = \frac{(1550e-9)^2}{1e-9} = 2.4\text{mm}$.

2.3 Optical Fibres

Single-mode fibres were used over multi-mode fibres as there is no inter-modal dispersion/smearing over long distances. Polarisation-maintaining (PM) fibres reduce cross talk between polarisation modes by ensuring different polarisation modes travel at different speeds, using stress rods to create birefringence (see figure 1). Most of the fibres used have 8° angled physical contact, this ensures that any reflection light at the interface is direction towards to wall at angle $< \theta_c$ so it is lost to the cladding.

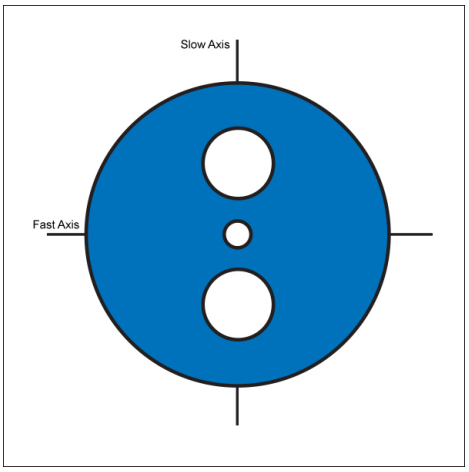

Figure 1: Pandas style polarisation maintaining fibres

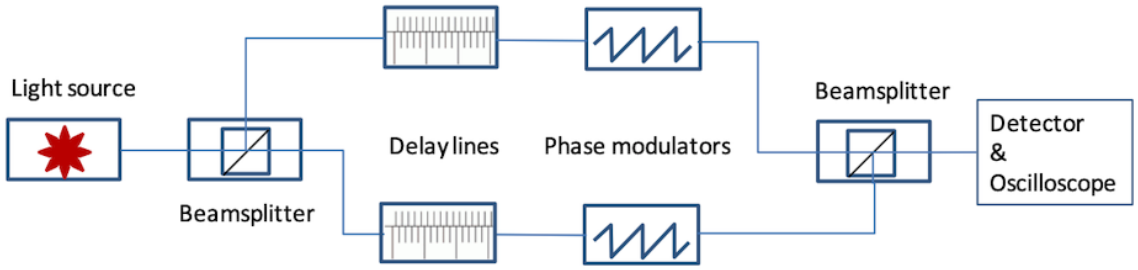

Figure 2: Mach-Zehnder Interferometer setup

2.4 Sources

A super-luminescent diode (SLD) and Fabry-Perot (FP) laser are used, both centred at 1550nm. Being a diode, the SLD has a short coherence length; whereas, the FP source is a laser meaning the output is highly coherent. 1550nm was a good wavelength to choose as this is the maximum power transfer for the fibre optic cables, so components would be more readily available.

2.5 Mach-Zehnder Interferometer

The amplitude-division interferometer consists of a single source spit by a 50:50 beamsplitter. After this, delay lines allow for changes in the length of each arm over a range of 25mm with precision ± 0.005mm. This is sufficient to explore the fringe behaviour considering the coherence lengths of the SLD and FP laser.

$LiNbO_3$ modulators are found in both arms of the interferometer to equalise path length - but only one is actually used. Due to the Pockels effect, the change in the refractive index of the modulator is proportional to the voltage across it, $\Delta\phi''(t) \propto V$.

A sawtooth driving signal causes $\Delta\phi''(t)$ to increase linearly with time, with an amplitude which can be adjusted to 2π to give continuous fringes. If the voltage is too low/high the max $\Delta\phi''(t)$

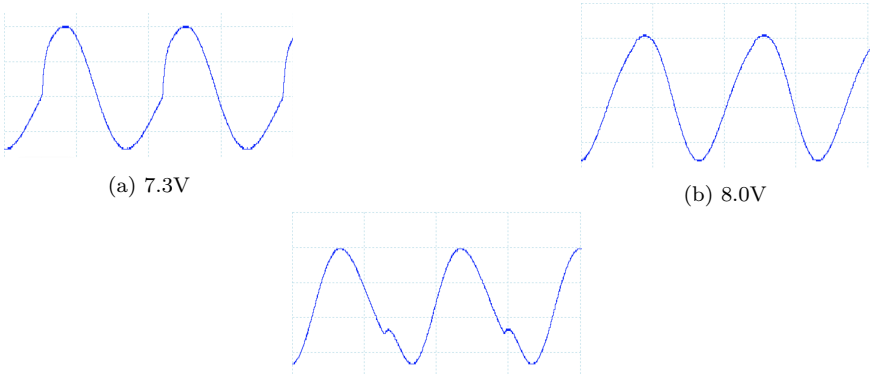

(a) 7.3V

(b) 8.0V

(c) 8.7V

Figure 3: fringes as signal generator p-2-p voltage is changed

will be less/greater than 2π leading to a discontinuities in the signal as seen in figure **??**. The rapid modulation ensures that point of maximum constructive and destructive interference are seen so fringe visibility can be found using equation 3. The modulator changes the path length by just one wavelength/2π where as even the smallest increment of 0.01mm on the delay line changes path length by 6.5 wavelengths. This demonstrates that the delay line is concerned with the spatial coherence length and the modulator is concerned with showing interference fringes at a point of a given coherence. After the modulator, the arms are rejoined at another 50:50 beamsplitter. Then there is an adjustable attenuator to ensure the InGaAs photodiode, doesn't get saturated.

The pump current of the amplifier powers a pump laser which has a wavelength of 980nm, exciting the erbium ions. Photons passing through the amplifier can cause stimulated emission of 1550nm photons, which are coherent with the incoming photons. As they are coherent they can contribute to the interference pattern, even though they were generated after the beamsplitter. Excited ions can spontaneously emit photons which are incoherent to incoming photon and are emitted isotropically. Some of these spontaneously emitted photons will be travelling in the same direction as the incoming photons, which are amplified by the same process of stimulated emission, these photons will contribute to the noise due to their incoherence with the incoming signal. Noise also increases with length of the cable.

2.6 Laser Vibrometer

2.6.1 Apparatus

The setup consists of a beamsplitter with the one arm heading into optical circulator, a three port device where light entering any port exits the next. The signal then leaves the fibre and bounces off mirror attached to a loudspeaker. The signal then goes back down the fibre and is recombined with the reference arm in the beamsplitter. 90:10 beamsplitters are used to account for greater losses in the arm that leaves the cable.

The loudspeaker is like a modulator as it oscillates, but now sinusoidally, and also like a delay line as the amplitude of oscillation is $\Delta\phi >> \lambda$. The fringes, see figure 5, look very similar to the pattern seen when you push the delay line over a few millimetres with your finger.

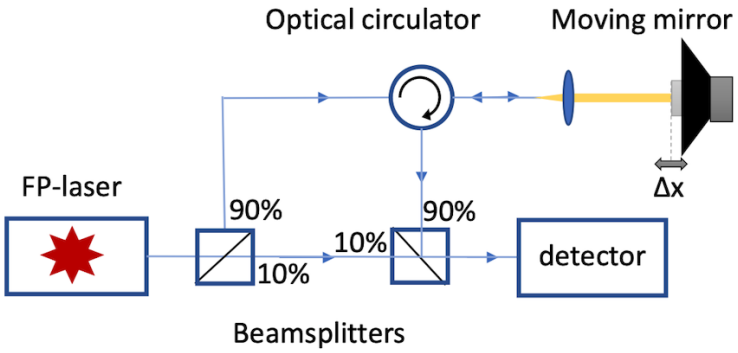

Figure 4: Laser Vibrometer

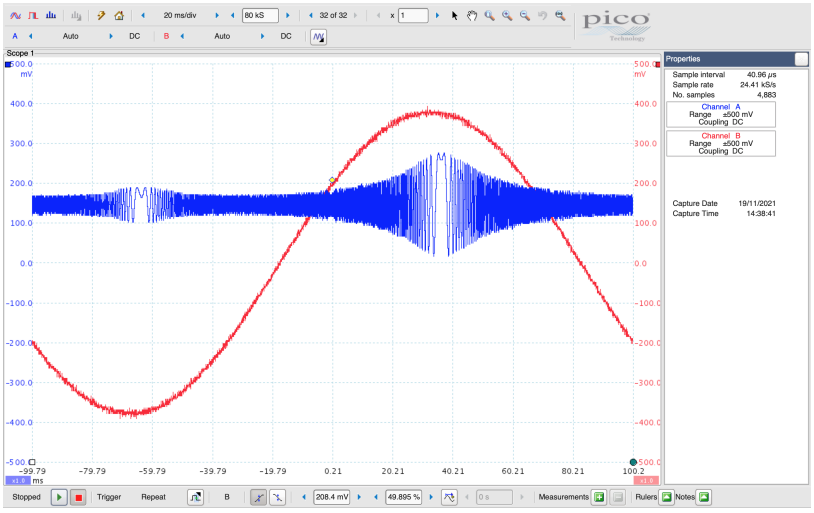

Figure 5: Laser vibrometer fringes

2.6.2 Doppler shift

Doppler shifting of the light from frequency, f, to frequency, f' occurs due to the moving loudspeaker. Using equation 2 the interference term becomes:

$$a_1 a_2 \cos[\Delta\phi - (\omega' - \omega)t] = a_1 a_2 \cos[\Delta\phi - 2\pi * (f' - f)t] = a_1 a_2 \cos(\Delta\phi - 2\pi\Delta f t) \tag{7}$$

This means the fringes oscillate with frequency, $\Delta f(t)$, therefore, for a suitably sized window around any point the dominating frequency should be $\Delta f(t)$. The relationship between $\Delta f(t)$ and velocity is derived in the appendix to give:

$$v = \frac{\Delta f * \lambda}{2} \tag{8}$$

Figure 5 shows the fringes, the large peak is when the mirror is closest to the fibre, as here more of the signal will go back into the fibre and the smaller peak is at the far position. At these points the velocity is zero, the frequency of the beats $\Delta f(t) = 0$, consistent with equation 8.

The output of the FFT is a complex value, but we want a real number, so take the absolute value using `np.abs(yf)`. This means that all the values measured are $|\Delta f|$. From data alone it is not possible to know what is positive and negative frequency. Although, it is trivial to reconstruct the Δf pattern by looking at the fringes and seeing whether that part of the cycle is travelling towards or away from the fibre.

3 Mach-Zehnder Interferometer

3.1 Method & Results

3.1.1 Optimising the equipment

Initially, the challenge was to equalise path lengths, the function generator was turned to 1KHz and 8V, then the contrast of the broad spectrum SLD was maximised by adjusting the delay lines. At the maximum, the bottom and top delay lines measured 2.16mm and 20.46mm respectively.

After this, the contrast was optimised by adjusting the SLD current and the signal generator voltage/frequency. It was found that 87.67mA was the best SLD current and for the signal generator optimum frequency was $\tilde{3}$00Hz and no discontinuities were seen in the fringes at $\tilde{8}$.0V, see figure 3b. This eventually gave a contrast of $\tilde{0}$.88.

3.1.2 Finding SLD Spectrum

The central maximum would drift slightly over time, up to a maximum of 0.05mm/hour, to reduce this impact measurements were taken quickly and carefully. To reduce systematic error due to the drift 10 measurements were taken above the maximum and then ten below [3] until 199 measurements were taken, 1.18mm to 3.08mm. Using 6 we can see that $\Delta\lambda =$ 1.3nm. This was good enough we we know changes in the spectrum happen on the order of nanometres. The minimum measurement spacing of 0.01mm was used as the SLD spectrum is wide in frequency space, meaning be able to use the approximations from section 2.2 we must have measurements close enough in real space, that they are far away enough in frequency space that the SLD spectrum repeats do not over. This gave the contrast-airgap graph seen in figure 6.

As per equation 5, to find the spectrum you must take the Fourier transform of the contrast-airgap relation.

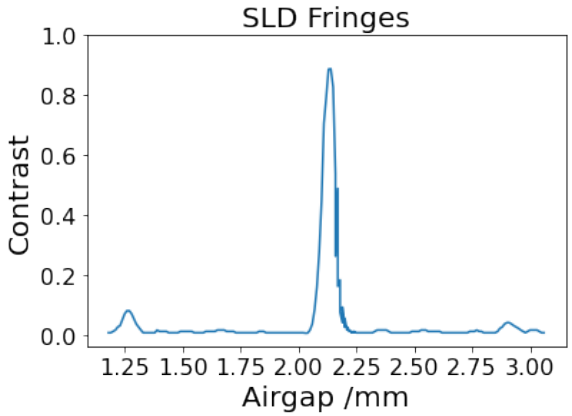

Figure 6: Super Luminescent Diode fringe pattern over a changing delay line length

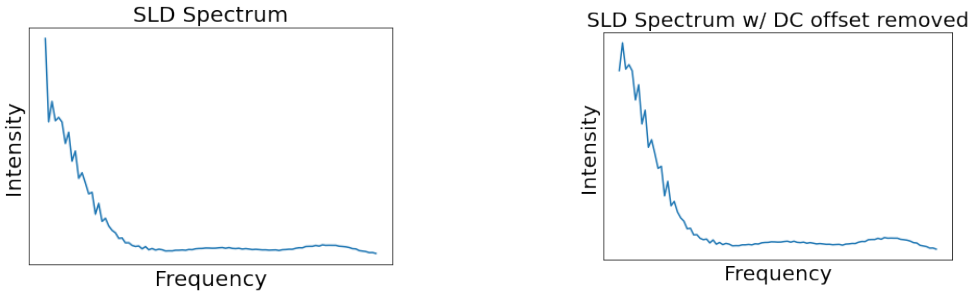

(a) (b)

Figure 7: Super Luminescent Diode Spectrum

As all values are real the Fourier transform will be symmetric meaning only values for $f > 0$ must be calculated. Using `scipy.rfft` instead of `scipy.fft` halves the amount of compute required, this isn't the bottleneck for analysis but is good practice.

The spectrum can be seen in figure 7, the initial plot had a peak at 0 corresponding to a DC offset, which vanishes when you remove the first element of the array. The spectrum is broad as expected but it was not possible to get quantitative values as the values for I_1 and I_2 would fluctuate throughout the measurement period.

3.1.3 Finding Fabry-Perot Laser Spectrum

The FP laser coherence length is much greater, so it was more important to have a large window to capture fringe contrasts further away from the central maximum and less important to have such tight measurements as the narrow spectrum means it won't overlap with a neighbouring repeat as easily.

Both arms were made 2mm longer allowing for a larger range in the bottom delay line. 202 measurements from 0.20mm to 8.24mm were taken yielding fig 8 for contrast-airgap relationship. The greater coherence length can be seen as the amplitude decay of the fringes is negligible over the range tested.

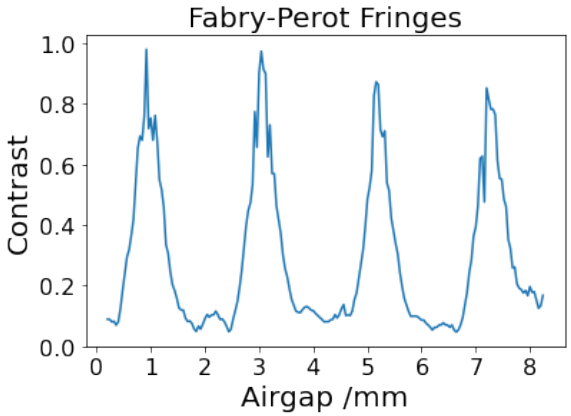

Figure 8: Fabry-Perot fringe pattern over a changing delay line length

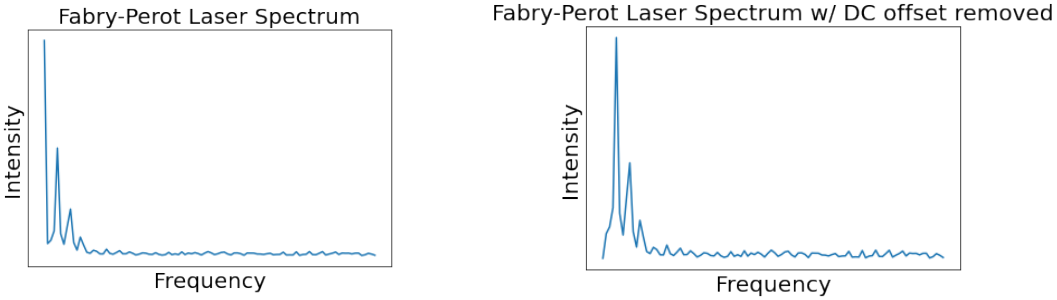

(a) (b)

Figure 9: Fabry-Perot Spectrum

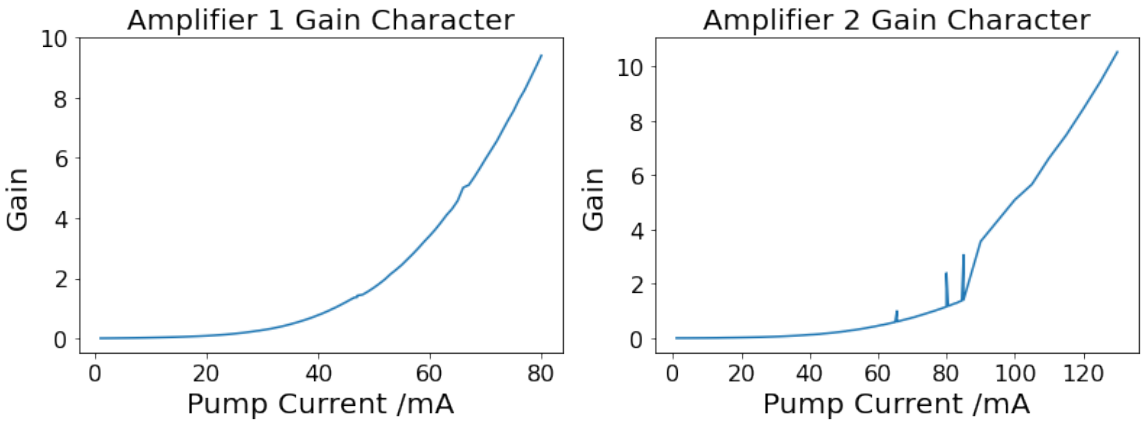

(a) (b)

Figure 10: Gain character for two amplifiers

The same method was used to find the spectrum and the DC offset was removed - see figure 9. Both spectra matched closely that given in the ThorLabs manual.

3.2 Spatial coherence lengths

The spatial coherence of the sources is defined as the distance at which the fringe contrast falls by a factor of e. For SLD the contrast was a $50 \pm 5\mu m$, which matches well with what is expected. The Fabry-Perot source has a much longer coherence length and its fringes were dropping slowly but didn't drop enough to give coherence length, which will be on order 100mm.

3.3 Polariser & Delay lines

Measurements were then taken to see the effect of the polariser and the airgap of the delay line. The contrast decreased by 24.1% when the polariser was removed which suggests significant cross talk between modes and potential that not all cables were PM. The strength of the signal with one arm blocked was measurement for both the minimum and maximum delay line length, giving 2.72V and 2.68V respectively, this is small enough to not affect the fringes.

3.4 Optical amplifier in one arm

Both amplifiers were characterised by measuring gain for over pump current (1-90mA) to yield figure 10. The signals were attenuated ~10x at 47mA and 80mA respectively to continue characterising without the photodiode getting saturated 12V. To equalise path lengths, cables were measured (the path length of the first amplifier is 3110mm), this led to a combination of the amplifier and cable in one arm (3110mm + 1055mm) and two cables in the other (2097mm + 2063mm), for a theoretical path difference of 5mm. Adjustment to the delay lines regained the SLD contrast maximum, the actual path length of the amplifier was calculated to be 3136mm. The amplifier characterisations were an interesting shape that turned out not to be exponential, as it initially looks.

Whilst left at the SLD contrast maximum, the contrast was measured as a function of amplifier pump current, which allowed the contrast-gain relationship to be plotted along side the theoretical

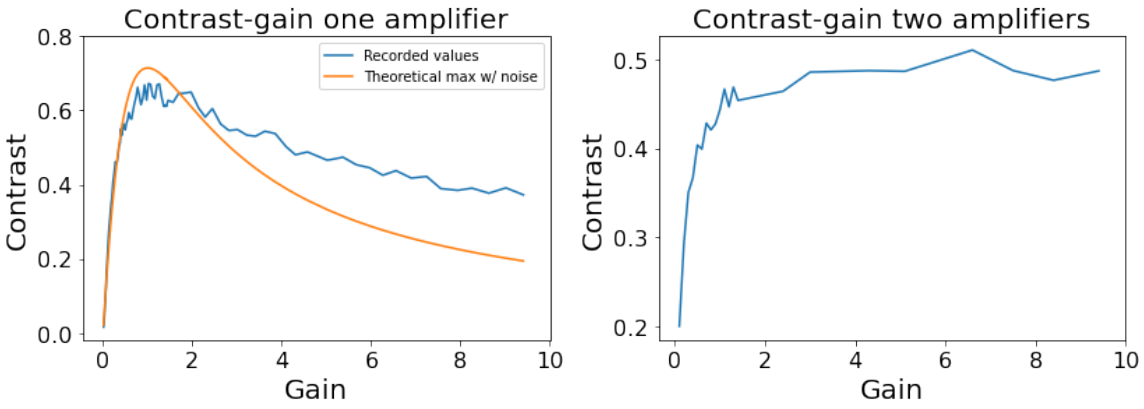

(a) One amplifier

(b) Two amplifier

Figure 11: Contrast against gain whilst using amplifiers

maximum contrast for a given level of noise (derived in appendix), seen in figure 11a.

As expected as expected the maximum contrast is at unity gain then decreases. The max contrast is 24.7% lower than that for no amplifier, due to the incoherent spontaneous emission that also gets amplified. The theoretical maximum contrast as a function of gain and noise is also plotted to see how well this model explains what is going on.

3.4.1 Optical amplifier in both arms

The second amplifier, which was marked as 120mm longer than the first, was added into the second arm and equalised,,

(1128 + 2152 + 3136=) 6416mm in the first arm and (1064 + 2097 + 3256=) 6417mm in the second arm. Using the figures 10a and 10b the gain was set to the same in both arms and steadily increased to give the contrast-gain results seen in figure 11b. Initially, the signal rises then flattens out as the noise is proportional to the gain.

The noise figure was measure by using the mean voltage over the standard deviation (PicoScope feature) both straight from the SLD and the SLD via the amplifier. This gave a NF value of 0.7 which is not reasonable.

3.5 Discussion

One of the biggest challenges throughout this experiment was the instability of the Fabry-Perot source, often changing rapidly or flickering, events like this would often come in waves. The best way to mitigate was to ensure that the source was allowed to warm up to a stable operating temperature. To improve, I would find methods of ensuring that the strength of the beams were both the same and constant. This would provide better measurements for the fringes and constant strengths for I_1 and I_2 meaning FFT plots would be quantitative. This would allow for the measurement of the FP laser cavity length. The resonant modes are multiple of half wavelengths so:

$$l = \frac{\lambda^2}{2\Delta\lambda} \tag{9}$$

Another method for measuring a spectrum is using a diffraction grating. For a grating fringe of order m, size W and slit separation D the resolution is given by:

$$\frac{|\Delta\lambda|}{\lambda} = \frac{D}{mW} \tag{10}$$

Like FTS, resolution will get better for a wider sampling region/grating. For a good grating (D = 100nm) the resolution is 10^{-8}m which is much worse than FTS. Diffraction gratings take one measurement from a multi pixel detector and FTS takes many measurements from a single pixel detector.

The fringes were very sensitive, to improve the repeatability of fringes cables equipment should be isolated where ever possible. Examples are: winding up cables so they are not hanging off the edge of the table, placing components that may vibrate/fluctuate in temperature (e.g. oscilloscope) far away or ensuring that components such as the beamsplitter are not subject to temperature fluctuations from environmental effects such as air currents.

When taking measurements the micrometer of the delay line had to be turned, the PicoScope read and then entered into an excel spreadsheet, all manually. This made measurements both tedious and time consuming. PicoScope have a SDK (software development kit) which, using the python API [5], can create scripts to record, for example, a measure of contrast every second to a spreadsheet. If this was using in conjunction with a motor rotating the delay line at a known angular frequency, results could be taken at known time intervals which could be mapped to displacement of the delay line.

- more things to investigate to ensure emission wasn't spontaneous

4 Interferometric Velocity Detection

The second part of the experiment was using a 'laser vibrometer' as seen in figure 4 using the FP laser. The 90:10 beamsplitters had a ratios of 9 ± 1 which was sufficient for the experiment.

4.1 Method & Results

The mirror was adjusted to ensure the signal was going back into the cable. Once a signal was seen, the loudspeaker was moved back to roughly equalise path lengths in each arm, although this is not so important as the FP laser has fairly large coherence length.

There were multiple powers for the FP laser that worked well at both 1.45 and 1.90. For the signal generator, 5Hz and 7V led to the sharpest and most stable peaks. Before results were saved from the PicoScope, the loudspeaker driving signal (red) was turned off as the number of samples that can be taken is a total for all channels so by turning off the second channel the number of samples doubled to 9970.

Taking FFTs over a number of windows and using 8 we can find the velocity as a function of time, A maximum of $\tilde{4}.0 \pm 0.1$mm/s was found. We can then find the amplitude by assuming velocity is constant over the regions between windows and performing a Riemann integral.

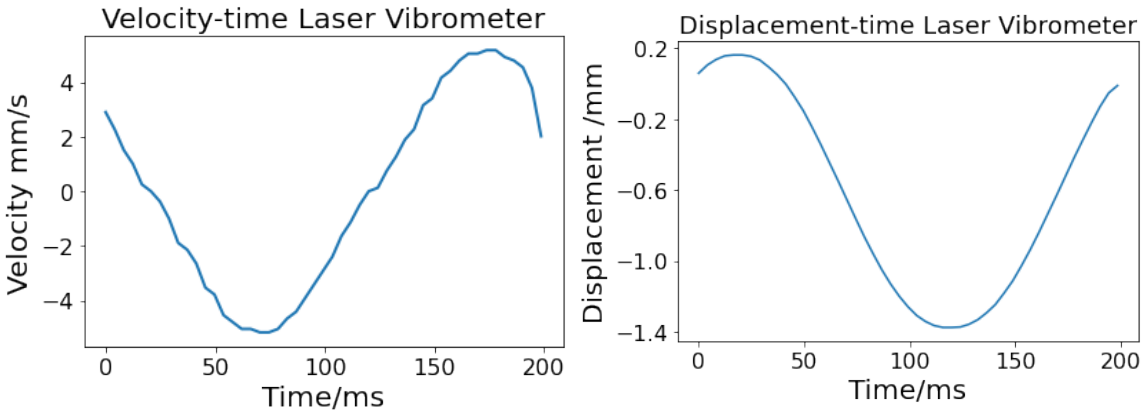

(a) (b)

Figure 12: Velocity and amplitude of the loudspeaker as functions of time

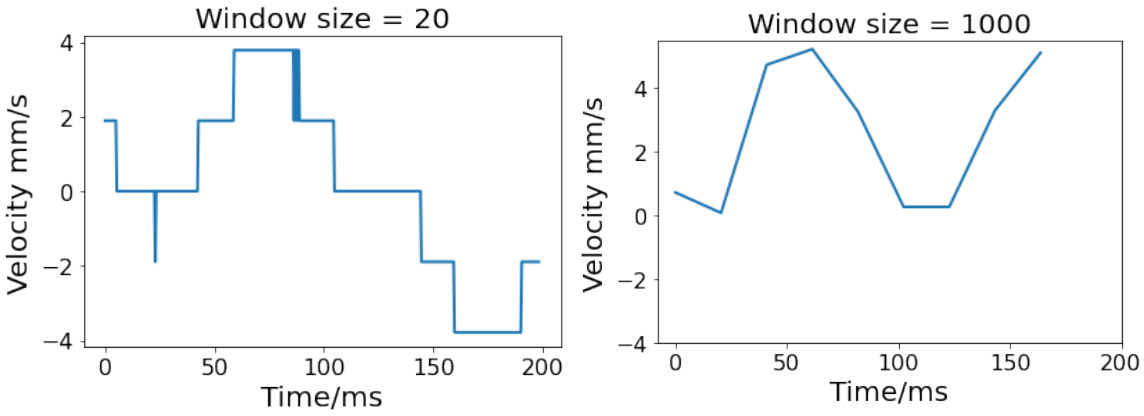

(a) Too small (b) Too large

Figure 13: Velocity-time if the windows are incorrect sizes

4.2 Discussion

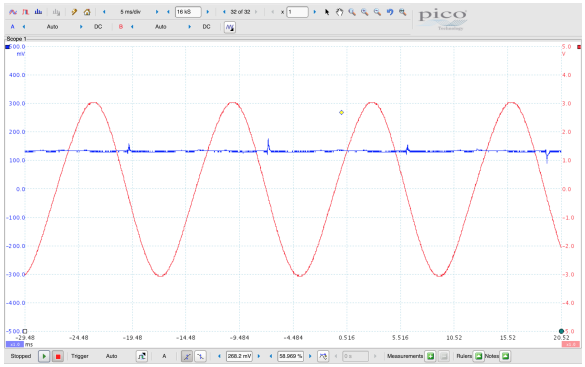

Figure 14: Near the resonance of the loudspeaker there is $\pi/2$ phase difference

Resonance effects can be seen in the laser vibrometer, at low driving frequencies, for example, 5Hz in 5, there is negligible phase difference between the driving and the fringes. But at 78Hz, for example, in figure 14, we can see that a $\pi/2$ phase difference which corresponds to resonance.

The PicoScope was limited to 50 kSamples/sec, it would be good to get a PicoScope capable of faster sampling. Top hat windows were used of size 300 data points, the optimal spacing between windows was 200. Figure 13 shows what happens if you have windows that are too small to properly see what the frequency components are e.g less than a cycle and too large that they don't accurately represent the frequency of that point.

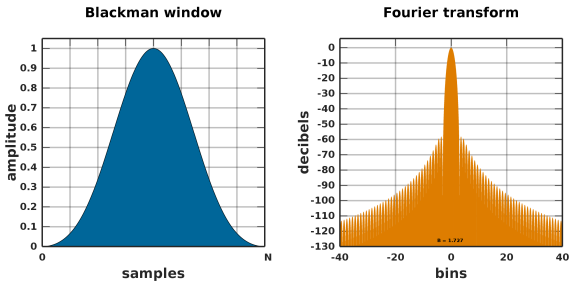

Figure 15: Blackman window and transform

Modified window functions are used to more accurately reproduce the underlying signal, these include the PicoScope's default Blackman window, which can be seen in figure 15.

5 Conclusion

The principal conclusions of this experiment are:

1. SLD and Fabry-Perot laser sources have very different spatial coherence lengths - seen in the fringes.

2. Amplifiers can increase the number of coherent, interfering photons by stimulated emission and add noise by spontaneous emission.

3. A first-order model for noise is good for modelling maximum contrast against gain.

4. Laser vibrometers are simple and effective in measuring velocity and amplitude for moving objects.

5. Different window functions are available to improve Fourier methods.

Overall, the experiment has shown different methods of measuring interference and analysis with FFT with scope for further exploration.

6 Appendix

6.1 Maximum Contrast Expression

It is known from equation 2 that:

$$\langle I \rangle \propto \frac{1}{2}\langle a_1^2 \rangle + \frac{1}{2}\langle a_2^2 \rangle + \langle a_1 a_2 \Re[e^{i[\Delta\phi - (\omega_1 - \omega_2)t]}] \rangle \tag{11}$$

Where $|\Re[e^{i[\Delta\phi-(\omega_1-\omega_2)t]}]| = 1$
Simplify the expression now and drop time averages (they are implied)

$$I_{\max/\min} \propto \frac{1}{2}a_1^2 + \frac{1}{2}a_2^2 \pm a_1 a_2 \tag{12}$$

Let $a_1 = ka_2$:

$$C(x) = \frac{I(x+x')_{\max} - I(x+x')_{\min}}{I(x+x')_{\max} + I(x+x')_{\min}} = \frac{2a_1 a_2}{a_1^2 + a_2^2} = \frac{2k}{1+k^2} \tag{13}$$

If we allow for a noise term C which is proportional to gain, k, we just add it on to the end of the expression as it increases the intensity but doesn't contribute to :

$$I_{\max/\min} \propto \frac{1}{2}a_1^2 + \frac{1}{2}a_2^2 \pm a_1 a_2 + kC \tag{14}$$

We now get a new, slightly modified expression, for the maximum contrast:

$$C(x) = \frac{2k}{1+k^2+2kC} \tag{15}$$

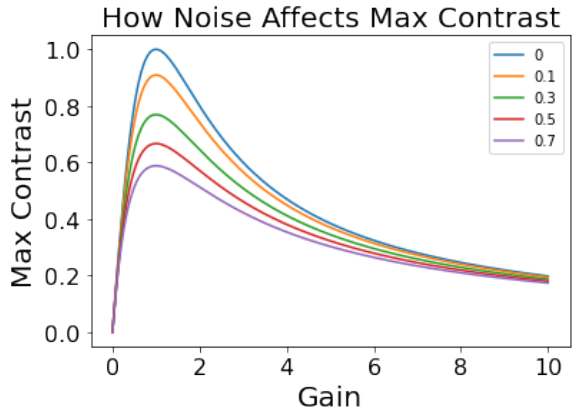

Figure 16: How noise changes the max contrast-gain relationship

6.2 Justification for assumption of continuous measurements

The measurement of the interference fringes, $I'(x)$, is equivalent to an infinite array of delta functions, $A(x)$, spaced however close the measurements are taken, multiplied by a top hat function, $W(x)$, which represents the range over which measurements are being made, multiplied by the fringe signal, $I(x)$.

$$B(x) = W(x) \times I(x) \tag{16}$$

$B(x)$ is the signal that would be measured if the sampling was continuous throughout the top hat. Using convolution theorem:

$$\tilde{B}(k) = \tilde{W}(k) * S(k) \tag{17}$$

$\tilde{B}(k)$ will be the spectrum function with of the true signal smeared out by a sinc function, $\tilde{W}(k)$, which becomes thinner, therefore less smearing, as the tophat becomes wider. Therefore now taking into account the array of deltas for non-contiuous sampling:

$$I'(x) = A(x) \times B(x) \tag{18}$$

Again using convolution theorem:

$$S'(k) = \tilde{A}(k) * \tilde{B}(k) \tag{19}$$

is also an array of delta functions, with its spacings being the inverse of that in real space. If the spacings in real space are close enough together, they are far enough apart in frequency space for the repeats of $\tilde{B}(k)$ to not overlap during convolution. So given that in this experiment the measurements are close enough so we can assume repeats of $\tilde{B}(k)$ don't overlap, therefore can say this is equivalent to continuous measurements.

6.3 Resolving Power of the Fourier Transform Spectrometer

The measured intensity $I'(x)$ over some window is equivalent to the true intensity over an infinite window multiplied by a tophat function $W(x)$

$$I'(x) = W(x) \times I(x) \tag{20}$$

Using convolution theorem:

$$S'(k) = \tilde{W}(k) * S(x) \tag{21}$$

For the width of blurring function in spatial frequency is $\Delta k = \frac{2\pi}{w}$. Using $k = \frac{2\pi}{\lambda}$ we can see that $\frac{dk}{k} = -\frac{d\lambda}{\lambda}$

Make sure i ref the lecture notes here

Therefore the resolution is [2]:

$$\frac{|\Delta\lambda|}{\lambda} = \frac{\Delta k}{k} = \frac{2\pi}{w}\frac{\lambda}{2\pi} = \frac{\lambda}{w} \tag{22}$$

6.4 Doppler Velocitometry

The standard expression for the frequency seen by an observer when the observer is moving at u and the source is moving at speed w.

$$f' = \frac{c+u}{c+w}f \tag{23}$$

In our situation we can say that if the loudspeaker is moving at speed v.

If you are in the frame of reference of the loudspeaker the observer is moving at a speed -v relative to the mirror. The value of u is -2v as the light has to travel twice the distance between observer and the mirror which is changing at speed -v.

$$f' = \frac{c-2v}{c}f \tag{24}$$

$$\Delta f = f' - f = \frac{-2v}{c}f = \frac{-2v}{\lambda} \tag{25}$$

References

[1] Tijmen Euser. *Coherence and information in a fibre inteferometer*. 2021.

[2] Tijmen Euser. *Oscillations, Wave and Optics, Part IB*. 2020-2021.

[3] Chris Haniff. *Experimental Methods, Part IB*. 2020-2021.

[4] Ludwig Mach. "Ueber einen Interferenzrefraktor". In: *Zeitschrift für Instrumentenkunde* 12 (1892), pp. 89–93.

[5] PicoScope Technologies. *Knuth: Computers and Typesetting*. URL: `https://github.com/picotech/picosdk-python-wrappers`. (accessed: 28.11.21).

[6] Ludwig Zehnder. "Ein neuer Interferenzrefraktor". In: *Zeitschrift für Instrumentenkunde* 11 (1891), pp. 275–285.